ISSN 8755-6839

SCIENCE OF **TSUNAMI HAZARDS**

Journal of Tsunami Society International

Volume 37 **Number 2** **2018**

SEISMICITY ANOMALIES OF M 5.0+ EARTHQUAKES IN CHILE DURING 1964-2015

T.A. Adagunodo[1*], K.D. Oyeyemi[1], O.S. Hammed[2], A.R. Bansal[3], J.O. Omidiora[4] & G. Pararas-Carayannis[5]

[1]Department of Physics, Covenant University, Ota, Ogun State, Nigeria
[2]Department of Physics, Federal University of Oye-Ekiti, Oye-Ekiti, Ekiti State, Nigeria
[3] CSIR-National Geophysical Research Institute, Hyderabad, India
[4]Department of Languages and General Studies, Covenant University, Ota, Ogun State, Nigeria
[5]Tsunami Society International, USA

[*]Corresponding mail: theophilus.adagunodo@covenantuniversity.edu.ng ; taadagunodo@yahoo.com

TSUNAMI SOCIETY INTERNATIONAL, 1741 Ala Moana Blvd. #70, Honolulu, HI 96815, USA.

SCIENCE OF TSUNAMI HAZARDS is a CERTIFIED OPEN ACCESS Journal included in the prestigious international academic journal database DOAJ, maintained by the University of Lund in Sweden with the support of the European Union. SCIENCE OF TSUNAMI HAZARDS is also preserved, archived and disseminated by the National Library, The Hague, NETHERLANDS, the Library of Congress, Washington D.C., USA, the Electronic Library of Los Alamos, National Laboratory, New Mexico, USA, the EBSCO Publishing databases and ELSEVIER Publishing in Amsterdam. The vast dissemination gives the journal additional global exposure and readership in 90% of the academic institutions worldwide, including nation- wide access to databases in more than 70 countries.

OBJECTIVE: Tsunami Society International publishes this interdisciplinary journal to increase and disseminate knowledge about tsunamis and their hazards.

DISCLAIMER: Although the articles in SCIENCE OF TSUNAMI HAZARDS have been technically reviewed by peers, Tsunami Society International is not responsible for the veracity of any statement, opinion or consequences.

Submit manuscripts of research papers, notes or letters to the Editor. If a research paper is accepted for publication the author(s) must submit a scan-ready manuscript, a Doc, TeX or a PDF file in the journal format. Issues of the journal are published electronically in PDF format. There is a minimal publication fee for authors who are members of Tsunami Society International for three years and slightly higher for non-members. Tsunami Society International members are notified by e-mail when a new issue is available. Permission to use figures, tables and brief excerpts from this journal in scientific and educational works is granted provided that the source is acknowledged. Recent and all past journal issues are available at: http://www.TsunamiSociety.org CD-ROMs of past volumes may be purchased by contacting Tsunami Society International at postmaster@tsunamisociety.org Issues of the journal from 1982 thru 2005 are also available in PDF format at the U.S. Los Alamos National Laboratory Library http://epubs.lanl.gov/tsunami/
WWW.TSUNAMISOCIETY.ORG

ISSN 8755-6839

SCIENCE OF TSUNAMI HAZARDS

Journal of Tsunami Society International

Volume 38 Number 2 2018

SEISMICITY ANOMALIES OF M 5.0+ EARTHQUAKES IN CHILE DURING 1964-2015

T.A. Adagunodo[1*], K.D. Oyeyemi[1], O.S. Hammed[2], A.R. Bansal[3], J.O. Omidiora[4] & G. Pararas-Carayannis[5]

[1]Department of Physics, Covenant University, Ota, Ogun State, Nigeria
[2]Department of Physics, Federal University of Oye-Ekiti, Oye-Ekiti, Ekiti State, Nigeria
[3] CSIR-National Geophysical Research Institute, Hyderabad, India
[4]Department of Languages and General Studies, Covenant University, Ota, Ogun State, Nigeria
[5]Tsunami Society International, USA
[*]*Corresponding mail: theophilus.adagunodo@covenantuniversity.edu.ng ; taadagunodo@yahoo.com ;*

ABSTRACT

The study of magnitude-frequency distribution of earthquake hazards in a region remains a crucial analysis in seismology. Its significance has varied from seismicity quantification to earthquake prediction. The analysis of seismicity anomalies of magnitude M => 5.0 earthquakes in Chile from 1964 to 2015 was undertaken by the present study with a view of reporting the trend of earthquake occurrences in the region. Chile has an area of about 756, 950 km^2 with an extensive coastline of approximately 6,435 kms. It is situated in a highly seismically and volcanically active zone with a long, narrow strip of land between the Andes Mountains to the east and the Pacific Ocean to the west. It borders Peru to the north, Bolivia to the northeast, Argentina to the east and the Drake Passage in the far south. Of a total of 3,893 earthquakes that have been documented historically, magnitudes Richter 5.0 to 5.9 represent 92.6%, magnitudes 6.0 to 6.9 represent 6.8%, magnitudes 7.0 to 7.9 represent 0.6%, and magnitudes 8.0 to 8.9 about 0.1%. The quantity of earthquakes (**a**-value) revealed an estimate of 8.4. The **b**-value was estimated using Gutenberg-Richter (GR) and the Maximum Likelihood Estimation (MLE) methods. The estimated **b**-value using GR and MLE methods are 0.97 and 1.1 respectively, with an estimated average **b**-value ≈ 1. The present studies supprort the conclusion that Chile is seismically very active and prone to the recurrence of moderate-to-great earthquakes in the future.

Keywords: b-*value, Gutenberg-Richter relation, Maximum likelihood estimation, Seismic zone, Seismicity, Triple junction, Earthquake, Chile, Tsunami*

Vol. 38, No. 2, page 130 (2018)

1.0 INTRODUCTION

Earthquakes occur in seismically active zones but also outside tectonic margins - as is the case of Nigeria. However, more frequently earthquakes occur along tectonic interplate margins (Awoyera et al. 2016; Adagunodo et al. 2018; Awoyera et al. 2017; Awoyera et al. 2017). Strong events can cause extensive loss of life, massive destruction to buildings and infrastructure and render thousands of people homeless. (Adagunodo and Sunmonu, 2015; Hammed et al. 2018). The seismicity of a region can be described in terms of frequency of occurrence and the type and magnitudes of measured historic events (Adagunodo et al. 2018). Often shallow earthquakes near coastal tectonic margins generate destructive tsunamis. The largest earthquake of the 20th century (with Moment magnitude Mw= 9.5) occurred on May 22, 1960 off the coast of South Central Chile. It generated one of the most destructive Pacific-wide tsunamis (Iida et al., 1967; Cox & Pararas--Carayannis, 1967). Near the generating area, both the earthquake and the tsunami were extremely destructive, particularly in the coastal area extending from Concepcion to the south end of Isla Chiloe. Huge tsunami waves measuring as high as 25 meters, arrived within 10 to 15 minutes after the earthquake, killing at least two hundred people, sinking all the boats, and inundating half a kilometer inland. There was extensive damage and loss of life at Concepcion, Chile's top industrial city (Pararas-Carayannis, 1968a; 1968b; 1969 a,b; Kanamori & Cipar, 1974).

1.1 Subduction of the Nazca Tectonic Plate with the South American Plate.

The geometry of the subduction process of the Nazca plate with the continent of South America, is quite complex and so is the geology and the seismicity of the western edge of South America. The inclination of the subduction underneath the South American plate has resulted to the segmentation of the intermediate-depth portion of the subduing Nazca plate into five sections. Three of these sections are characterized by the subduction zone steeply dipping, while the other two have nearly near-horizontal subduction. The angle of dip ranges from 25^{o} to 30^{o} for the subdued Nazca plate into the mantle beneath southern Peru to northern Ecuador down to the northern and the southern Chile (USGS Earthquakes, 2015). In the vicinity of the 2015 Illapel earthquake the Nazca plate moves relative to South America in the east-to-northeast direction at velocity of 74 mm/yr[-..]

Though the South America plate is characterized by a chain of several active volcanoes due to the subduction process of the Nazca oceanic lithosphere alongside its partial melting along the arc, the regions with relatively inferred shallow subduction are characterized by absence of volcanic activity (USGS Earthquakes, 2015). Several previous studies of the orogenic and tectonic activities around Chile together with the tectonic framework of Chile have been reported by Pararas-Carayannis, (1960; 2010), and Dzierma et al. (2012). Generally, examination of earthquakes along the Nazca-South America convergence margin of Chile's northern end of the central seismic region are indicative of the complexity in the moment release, which can be correlated to structural variations within the subducting and overriding plates. The anomalous interactions affect crustal displacements and, therefore, the source characteristics of tsunamis that can be generated from large scale, thrust and reverse thrust seismic events in the region - nucleated by offshore compressional

earthquakes (Pararas-Carayannis, 2010). A study of preceeding smaller magnitude earthquakes – such as the ones described by the present study - can help determine a process of nucleation of a major fault where a major or great earthquake could occur in the future.

1.2 Seismicity of Chile

In the form of introduction, it is important to discuss briefly the seismicity of Chile, some of the most recent great earthquakes, but also the significance of the lesser magnitude events in helping forecast future larger magnitude events. As it is well established, the continuous crustal deformation associated with ridge collision and the oblique convergence of the Nazca tectonic plate with the continental block of South America, has caused substantial deformation and strain accumulation in Chile which culminates in great and major earthquakes and tsunamis (Figure 1). Both the oceanic crust and lithospheric portion of the Nazca plate are involved in this subduction activity, which caused the uplift of the Andes Mountains, thus resulting also in the formation of a large and active volcanic belt (USGS Earthquakes). The historic record documents numerous destructive earthquakes and tsunamis in Chile for over four hundred years. Most of the destructive earthquakes had focal depths generally less than 60 km (Zaytsev et al. 2016). The record shows that from 8 February 1570 - when a great tsunamigenic 1960 earthquake occurred near Concepcion - to the 16 September 2015 Illapel earthquake there was extensive destruction of property and 60, 894 people lost their lives.

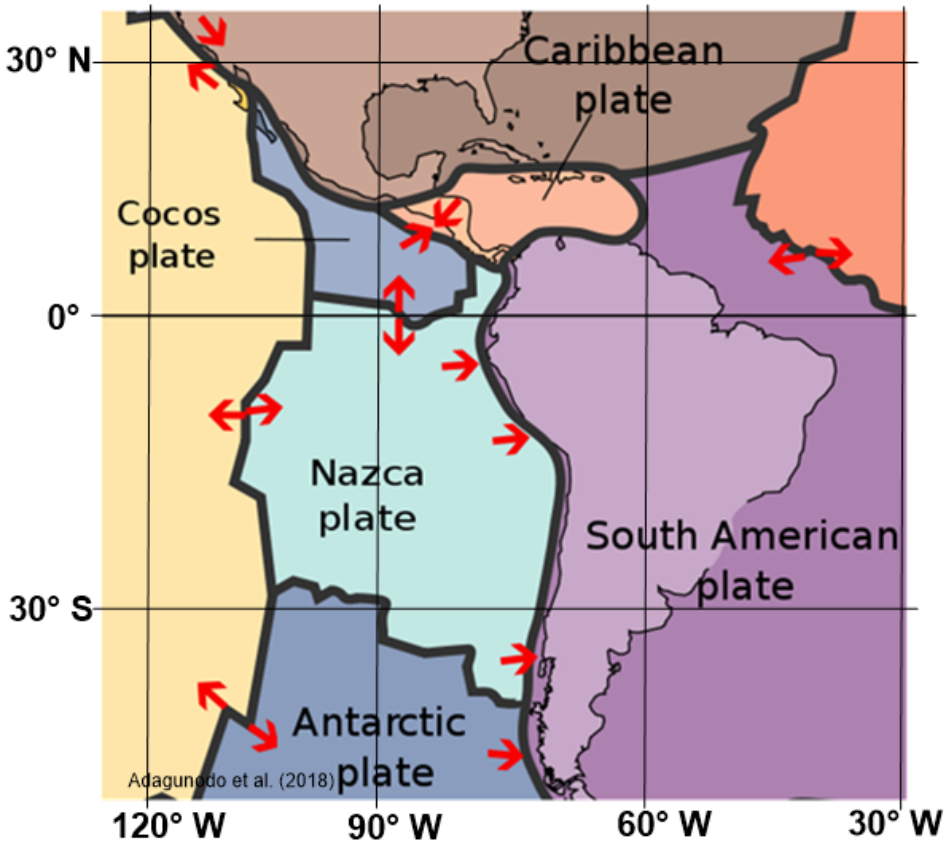

Figure 1: The South American Plates.

1.2 Historical Major and Large Tsunamigenic and NonTsunamigenic Earthquakes in Chile

Table 1 (at the end of Section 1.2) provides a list of historical earthquakes in Chile beginning with a great earthquake in 1570. Some of these earthquakes generated destructive local and Pacific wide tsunamis. All occurred along the tectonic interface between the Nazca and the South American plates. Many more significant events occurred before 1570 but there are no documented records. The greatest in magnitude M_w 9.5 earthquake in recent history occurred on May 22, 1960. It generated a destructive, Pacific-wide tsunami (Pararas-Carayannis, 2010a). More recently, another great tsunamigenic earthquake occurred on February 27, 2010. It had a Moment Magnitude M_w 8.8 (Pararas-Carayannis, 2010a) and generated a tsunami with a maximum wave of 8.6 feet which resulted in the destruction of several coastal villages along a coastline of about 596 km in length. The tsunami alone was responsible for about 500 deaths. The combined impact of the earthquake and the tsunami rendered homeless approximately 1.8 million people.

A large vigorous aftershock sequence followed the main earthquake and there was an unusual clustering and spatial distribution of aftershocks of all amplitudes. An aftershock of M 6.2 was recorded 20 minutes after the initial quake. A 6.9 magnitude offshore earthquake struck approximately 300 kilometers southwest less than 90 minutes after the initial shock; however, this may have been a separate event that may not have been related to the main shock. Two more aftershocks with magnitudes 5.4 and 5.6 followed within an hour. In the 2 1/2 hours following the 90-second main shock, 11 more were recorded. By March 1, 2010, a total of 121 aftershocks with magnitude 5.0 or greater were recorded (USGS NEIC). Eight of these had magnitudes of 6.0 or greater. By March 29, 2010, a total 458 aftershocks had been recorded (Pararas-Carayannis, 2010a).

Further evaluation of the source mechanism of tsunami generation associated with this earthquake of February 27, 2010 in Chile - as inferred from geologic structure, rupturing process, seismic intensities, spatial distribution of aftershocks, energy release and fault plane solutions - indicated that heterogeneous crustal displacements took place along the entire 550 km. earthquake rupture. As stated, the anomalous earthquake rupturing in opposing directions probably had a diminishing effect on tsunami generating efficiency. Also, since more significant vertical displacements of the ocean floor occurred in the region north of Concepción, most of the tsunami energy was generated in this region. A good portion of this energy was trapped, ducted or reflected by prominent submarine features such as the Juan Fernández Ridge, the O'Higgins seamount - thus lessening the tsunami's far-field impact by redirecting or deflecting its energy (Pararas-Carayannis, 2010a). Thus, the crustal displacements and energy, which contributed to tsunami generation, needed to be better determined and quantified, and such study was undertaken.

A comparison was made of similarities and differences of the source characteristics of the February 27, 2010 tsunami with those of the destructive, Pacific-wide tsunami of May 22, 1960 (Pararas-Carayannis, 2010a). The analysis was also useful in indicating the significance of the lesser events in the prediction of larger destructive earthquake is the future – thus also supporting the need for the present study. Comparison of the source characteristics of the 1960 and of the 2010-tsunamigenic

earthquakes showed differences in energy release, geometry of subduction, angle of dip and extent of crustal displacements on land and in the ocean. Also, there were significant differences in coastal geomorphology, spatial distribution of hypocenters, clustering, of time sequence of aftershocks and of seismic gaps at depth.

On April 1, 2014, another great Mw 8.2 shallow earthquake (25km focal depth) struck Chile. Its epicenter was about 95 km northwest of Iquique, caused extensive destruction and generated a tsunami with waves up to 2 meters which struck coastal Chile's coastal zone (USGS Earthquakes, 2015). .

On September 16, 2015 another tsunamigenic earthquake occurred near the coast of Illapel in Central Chile, as shown in Figure 1. The tsunami generated by this event was large and also caused severe damage to coastal villages. The quake had a seismic moment release of 3.2 x 10^{28} dyn-cm, corresponding to Moment Magnitude of M_w = 8.3 (Lin et al., 2016). The initial quake motions lasted for three minutes and several aftershocks followed with magnitude greater than six.

As it has been postulated for Peru and Chile, the angle of subduction of the Nazca oceanic plate beneath South America is not uniform along the entire segment of the Peru-Chile Trench. Furthermore, the relatively narrow zone of subduction is affected by buoyancy forces of the bounding oceanic ridges and fractures and is characterized by shallow earthquakes that can generate destructive tsunamis of varied intensities (Pararas-Carayannis, 2012). Specifically, the Nazca plate is moving towards the east-northeast at a velocity of 74 mm/yr with respect to South America and begins subducting beneath the continent, 85 km to the west of the area which was affected by the 16 September 2015 earthquake. The size, location, depth and mechanism of this event in central Chile, are all consistent with its occurrence on the megathrust interface in this region. The anomalous, rupturing in opposing directions probably had a diminishing effect on tsunami generating efficiency (Pararas-Carayannis, 2012).

In summary, subsequent studies of smaller magnitude aftershocks and of past historical events of all magnitudes are indicative of earthquakes in each of Chile's three main seismic regions, of the extent of ground and ocean floor displacements, of the aftershock hypocenter space/time distribution, of the geometry of subduction, of the quakes' tsunamigenic efficiency, of the expected tsunami energy flux directivity, of the absorption, of trapping, of reflection and of ducting of wave energy and, finally, of the potential for future destructive earthquakes and tsunamis in Chile. Table 1 is a list of all known earthquakes.

Table 1: List of tsunamis/earthquakes in Chile (Adapted from WikiProject Earthquakes, 2017).

Location	Date	Magnitude	Type	Depth (km)	Death Toll
Concepcion	February 8, 1570	8.3	Ms		
	March 17, 1575	7.3	Ms		
Valdivia	December 16, 1575	8.5	Ms		
Offshore Arica	November 24, 1604	8.5	Ms	30	
Offshore Arica	September 16, 1615	8.8	Ms		
Santiago	May 13, 1647	8.5	Ms		
	March 15, 1657	8.0	Ms		
	March 10, 1681	7.3	Ms		
	July 12, 1687	7.3	Ms		
Valparaiso	July 8, 1730	8.7	Ms		5
	December 24, 1737	7.7	Ms		
Concepcion	May 25, 1751	8.5	Ms		
	March 30, 1796	7.7	Ms		
	April 11, 1819	8.3	Ms		
Valparaiso	November 19, 1822	8.5	Ms		200
	September 26, 1829	7.0	Ms		
	October 8, 1831	7.8	Ms		
	September 18, 1833	7.7	Ms	60	
Concepcion	February 20, 1835	8.5/8.2	Ms/$M_?$		500
	November 7, 1837	8.0	Ms		
	October 8, 1847	7.3	Ms		
	December 17, 1849	7.5	Ms		
	December 6, 1850	7.3	Ms		
	April 2, 1851	7.1	Ms		
	October 5, 1859	7.6	Ms		
Arica	August 13, 1868	9.0/8.5	$M_?$/Ms		25, 000
	August 24, 1869	7.5	Ms		
	October 5, 1871	7.3	Ms		
Iquique	May 9, 1877	8.8	Ms/$M_?$		34
	January 23, 1878	7.9	Ms	40	
	February 2, 1879	7.3	Ms		
	August 15, 1880	7.7	Ms		
Valparaiso	August 16, 1906	8.2	Mw	25	3, 882
	June 8, 1909	7.6	Ms		

	October 4, 1910	7.3	Ms		
	September 15, 1911	7.3	Ms		
	January 29, 1914	8.2	Ms		
	February 14, 1917	7.0	Ms		
	May 20, 1918	7.9	Ms		
	December 4, 1918	8.2	Ms	60	
	March 1, 1919	7.2	Ms	40	
	March 2, 1919	7.3	Ms	40	
	December 10, 1920	7.4	Ms		
	November 7, 1922	7.0	Ms		
Vallenar	November 10, 1922	8.5	Mw	25	
	May 4, 1923	7.0	Ms	60	
	May 15, 1925	7.1	Ms	50	
	April 28, 1926	7.0	Ms	180	
	November 21, 1927	7.1	Ms		
	November 20, 1928	7.1	Ms	25	
Talca	December 1, 1928	8.3/7.6	Ms/M?		225
	October 19, 1929	7.5	Ms	100	
	March 18, 1931	7.1	Ms		
	February 23, 1933	7.6	Ms	40	
	March 1, 1936	7.1	Ms	120	

	July 13, 1936	7.3	Ms	60	
Chillan	January 24, 1939	8.3/7.8	Ms/M?	60	28, 000
	April 18, 1939	7.4	Ms	100	
	October 11, 1940	7.0	Ms		
	July 8, 1942	7.0	Ms	140	
	March 14, 1943	7.2	Ms	150	
Ovalle	April 6, 1943	8.2	Mw	55	25
	December 1, 1943	7.0	Ms	100	
	July 13, 1945	7.1	Ms	100	
	August 2, 1946	7.9	Ms	50	
	April 19, 1949	7.3	Ms	70	
	April 25, 1949	7.3	Ms	110	
	May 29, 1949	7.0	Ms	100	
Tierra del Fuego	December 17, 1949	7.8	Ms	30	

	December 17, 1949	7.8	Ms		
	January 29, 1950	7.0	Ms		
	December 9, 1950	8.3	Ms	100	
	May 6, 1953	7.6	Ms	60	
	December 6, 1953	7.4	Ms	128	
	February 8, 1954	7.7	Ms		
	April 19, 1955	7.1	Ms		
	January 8, 1956	7.1	Ms	11	
	December 17, 1956	7.0	Ms		
	July 29, 1957	7.0	Ms		
	June 13, 1959	7.5	Ms	83	
Concepcion	May 21, 1960	7.9/7.3	M_η/Ms		125
	May 22, 1960	7.3	Ms		
Valdivia	May 22, 1960	9.5/8.3	Mw/Ms	33	1, 655
	June 19, 1960	7.3	Ms		
	November 1, 1960	7.4	Ms	55	
	July 13, 1961	7.0	Ms	40	
	February 14, 1962	7.3	Ms	45	
	August 3, 1962	7.1	Ms	107	
Taltal	February 23, 1965	7.0	Ms	36	1
La Ligua	March 28, 1965	7.4	Ms	68	400
	December 28, 1966	7.8	Ms	23	
	March 13, 1967	7.3	Ms	33	
	December 21, 1967	7.5	Ms	33	
	June 17, 1971	7.0	Ms	76	
Illapel	July 8, 1971	7.5	Ms	40	90
	August 18, 1974	7.1	Ms	36	
	May 10, 1975	7.7	Ms	6	
	November 29, 1976	7.3	Ms	82	
	August 3, 1979	7.0	Ms	49	
	October 16, 1981	7.5	Ms	33	
	October 4, 1983	7.3	Ms	14	
Algarrobo	March 3, 1985	8.0/7.8	Mw/Ms	33	177
Rapel Lake	April 8, 1985	7.5	Ms	37	1
Iquique	March 5, 1987	7.3	Ms	62	
	August 8, 1987	7.1	Ms	42	
Antofagasta	July 30, 1995	8.0	Mw	47	3

Punitaqui	October 15, 1997	7.1	Mw	56	8
Near coast northern Chile	January 30, 1998	7.1	M?	42	1
Chile-Argentina	June 18, 2002	6.6	M?		
Border region near coast of central Chile	June 20, 2003	6.8	M?	12.8	

Biobio	May 3, 2004	6.6	Mw	21	
Tarapaca	June 13, 2005	7.8	Mw	108/117.2	11
Tocopilla	November 14, 2007	7.7	Mw	47.7/40	2
Antofagasta	December 16, 2007	6.7	Mw	57.8	0
Tarapaca	February 4, 2008	6.3	Mw	32.3	
Papudo	December 18, 2008	6.3/5.9	Mw/M_L	24.8/35	0
Offshore Tarapaca	November 13, 2009	6.5	Mw	28	0
Drake Passage	January 17, 2010	6.3	Mw	10	0
Offshore Maule/Biobio	February 27, 2010	8.8	Mw	30	525
Pichilemu	March 11, 2010	6.9	Mw	11/33.1	1
Araucania	January 2, 2011	7.1/6.9	Mw/M_L	25.1/32.1	0
Talca	March 25, 2012	7.1/7.0	Mw/Mw	34.8/40.7	1
Coquimbo	October 31, 2013	6.5	Mw/M_L	10.0	
Iquique Offshore Tarapaca	March 16, 2014	7.0	Mw	20.6	
Iquique Offshore Tarapaca	April 1, 2014	8.2	Mw	25	7
Iquique Offshore Tarapaca	April 1, 2014	7.5	Mw	26.8	
Iquique Offshore Tarapaca	April 1, 2014	7.0	Mw	29.7	
Iquique Offshore Tarapaca	April 2, 2014	7.7	Mw	22.4	
Valparaiso	August 23, 2014	6.4	Mw	32	
Easter Island	October 8, 2014	7.0	Mw	16.5	
Talcahuano Offshore Biobio	March 18, 2015	6.3	M_L	13	

Arica and Parinacota	March 23, 2015	6.4	Mw	130	
Illapel	September 16, 2015	8.3	Mw	25	15

1.3 Seismic Stress Tranference

Based on localized crustal movements in Chile, as well as on the oblique convergence of tectonic plates, it would be expected that seismic stress would be distributed, not only between the interphases of subduction, but also along the major faults within the overriding plate. However, as indicated by the earthquake of 12 January 2010 in Haiti, Coulomb Stress became evident in the adjacent segment of the local seismic zone and such progression of stress may culminate in the future to a potential rupture and a larger more destructive earthquake in Haiti (Pararas-Carayannis, 2010, b), but the same seismic stress transference occurs also in Chile and elsewhere along major faults.

Based on such analysis, it is apparent that oblique plate convergence contributes significantly to the build up of seismic stress transference and built up of strain in Chile. In the last five decades since 1960, crustal deformation from continuous plate convergence and subduction apparently has been building strain in the region. Although some of the strain has been released partially by smaller and some larger events and has been partially accommodated elastically, a great deal more strain is still accumulating. When the threshold limits of crustal elasticity are exceeded again in the region, another great earthquake can be expected to occur.

In summary, the build up in strain along regions of a subduction zone eventually requires released in the form of large horizontal and vertical crustal movements that restore temporarily isostatic balance. Thus, independent smaller events may release remaining strain in seismic zones or may nucleate transference of stress to adjacent segments of a seismic zone. Based on the experience gained by the study of the smaller events - as in the present study - makes it safe to conclude that such seismic transference occurs and future earthquakes in Chile will occur and may generate tsunamis with destructive near and far-field effects (Pararas-Carayannis, 2010).

1. 4 Recurrence Frequencies of Great Earthquakes

Estimating the recurrence frequencies of great earthquakes - based on slip rates - along the southern segment of Chile's central seismic region, is possible but not very accurate. Apparently, the 1960 tsunamigenic earthquake ended a recurrence interval that had begun almost four centuries before, in 1575. Two later earthquakes in 1737 and 1837 produced little subsidence or tsunamis and probably left a great deal of strain in this region from accumulated plate motion that was released subsequently by the 1960 earthquake (Cisternas et. al., 2005; Pararas-Carayannis, 2010). For example, based on the intervals of the destructive earthquakes of 1575, 1737, 1837 and 1960, the recurrence frequency for the Valdivia segment of Chile's southern seismic segment has been estimated at 128 ± 31 yr. Also, historic records of subduction earthquakes show that Isla Santa María is within the southern part of

the Concepción seismic segment (Lomnitz, 1970; Barrientos, 1987; Beck et al., 1998; Campos et al., 2002), which nucleated M> 8 subduction tsunamigenic earthquakes in 1570, 1657, 1751 and 1835 (Lomnitz, 1970, 2004; Melnick et al., 2006; Pararas-Carayannis, 2010). Thus, it can be concluded that the study of smaller magnitude earthquakes is important in illustrating how faulting and oblique compression along the seismogenic zone nucleates subduction and eventually results in the generation of destructive tsunamigenic and non-tsunamigenic earthquakes (Pararas-Carayannis, 2010),

Finally, it is quite possible that the strain release from the recent earthquakes may have accelerated the recurrence of another great tsunamigenic earthquakes along the southern and other seismic segments of Chile. Such event(s) could occur in a few decades from now or much sooner along the same rupture zone as that of 1960 or to the north of this zone. However, the use of new technology based on GPS geodetic measurements can help assess tectonic plate movements and slip rates. Such measurements may eventually lead to more accurate estimates of the recurrence frequency of great tsunamigenic earthquakes along Chile's north, central and south seismic zones.

In summary, besides measuring slip rates, there are several additional ways to help estimate the occurrence of future earthquake, based on focal depth analyses, magnitudes of events and expected seismic moments, as well as estimates of expected tsunami heights and other parameters (Abe, 1979; Aida, 1978; Yamashita and Sato, 1974; Pararas-Carayannis, 2010; Bolshakova and Nosov, 2011; Lay et al., 2011; Zaytsev et al. 2016). The combined oblique convergence of major ridge collision and the subduction process play important roles in pre-seismic strain accumulation and must be taken into account in predicting future great tsunamigenic earthquakes along Chile's seismic zones and elsewhere in the world (Pararas-Carayannis, 2010). The gradient in obliquity of convergence is also a significant factor in slip rates, crustal deformation and in the creation of fore-arc slivers, which may extend or contract parallel to the major tectonic arc.

1.5 Scope of the Present Study

The impact of earthquake and tsunami destruction can be studied through analysis of past and present earthquake events (Darwin, 1845; Alabi et al. 2013) - however, most of the historical catalogs are incomplete for such analysis (Pulama, 2004). For example, the catalog adopted for this study recorded its first event of an M 5.0 earthquake in Chile on February 6, 1963. This reduced the coverage period to 52 years. However, the aim and scope of the present study is to analyze the trend of earthquake anomalies of M equal or greater than 5.0 in Chile using the least square inverse method and the maximum likelihood method. To achieve this, the frequency distribution of individual magnitude within a time interval is analyzed, and the **b**-value of the study area is determined. Silbergleit and Prezzi (2012) analyzed earthquake data from 1900 to 2010 for Chile. Their statistical analysis suggested possible occurrence of major earthquakes in Chile with a Richter magnitude between 8.7 and 8.9 within the next decade. Reyes et al. (2013) used neural networks to predict the future occurrence of earthquakes in Chile. Their networks were capable to predict earthquake occurrence for five consecutive days. Some recently published articles on trend analysis of earthquakes of an area in

the world include: Nuannin et al. (2012), El-Isa and Eaton (2014), Han et al. (2015), Awoyera et al. (2016a), Awoyera et al. (2016b), Ismail-Zadeh et al. (2017), Nava et al. (2017), Olokoyo et al. (2017), Awoyemi et al. (2017) and Adagunodo et al. (2018).

The present study examines the region of Chile on the Western South American continent from 15^{o} to 55^{o} South latitude, and ranging from 75^{o} to 65^{o} W in longitude. The South American arc, which is about 7,000 kms, runs through the triple junction offshore within the Chilean margin to the Panama Fracture zone intersection in Central America. The area is localized within the boundary of the convergent plate tectonics between the Nazca and South America, which has resulted in varying degree of subduction.

Several of the historical earthquakes of larger magnitude along the coastal zone of South America are limited to shallow focal depths (0–70 km) due to shallow crustal deformations. These deformations and orogenic activities are the main causes of earthquakes within the overriding South American plate upon the Nazca plate that produce earthquakes with focal depth of up to about 50 km. However, interplate earthquakes with focal depths ranging between 10 and 60 kms are also common and are generated within slip faults along the dipping boundary separating the South America and Nazca plates. Internal deformations within the subducting Nazca plate often result in large intermediate-depth earthquakes within the ranges of focal depth approximately 10 to 300 kms. These are limited in size and their spatial extent often run inland into the continent of South America, but clusters form generally beneath SW Bolivia, northern Chile, northern Peru, and southern Ecuador, with focal depths ranging from 112 to 130 Kms. Several of the larger, shallow depth earthquakes are localized in the coastline region between Peru and Chile and have generated destructive tsunamis.

2.0 MATERIALS AND METHOD

The data used in this study was made available through the collaborative project of the United States Geological Survey and the University of California Berkley Seismological Laboratory. All the parameters of the earthquakes such as the time of occurrence, epicenter coordinates, time of origin, and the magnitude of the event are available for each datum. The data was also archived in the world catalogue of the Advanced Natural Seismic Source. As stated, the study area is situated between latitude 55^{o} to 15^{o} S and longitude 75^{o} to 65^{o} W in the Western South America. The data span through a 52-year period, from 1964 to 2015 amounts to 3,893 events. The minimum magnitude selected in the catalog search is 5.0 (light earthquake which results to some property damage) and the maximum magnitude is 9.0 (great earthquake near total destruction which result to total destruction of lives and properties) as revealed in Figure 2 belos. It shows representation of Richter scale earthquake magnitudes and energy equivalents complied by Bravo and Ortiz (2005). Chile and Haiti earthquakes were modified to Figure 2 from Andrea *et al*. (2011) while 2015 Illapel earthquake was added to the figure by the authors of the present study.

The relationship between the earthquake frequency and magnitude is prerequisite to assessing and evaluating the seismic activity in an area (Ghosh, 2007). Also, the relationship between the earthquake size distributions over a large range of magnitudes in a seismogenic volume can be

quantified and evaluated using a power law equation (Abercrombie, 1995; Alabi *et al*., 2013; Adagunodo et al. 2018). This relationship was first discovered in 1939 in Japan, followed closely by Gutenberg and Richter (1944) in California. Generally, the Gutenberg – Richter (GR) law and is presented in Eq. (1).

$$\mathrm{Log}_{10}N(M) = a - bM \qquad (1)$$

where N(M) is the events' number with magnitude greater than or equal to M, and a and b are constants that vary in time and space. In some conditions, log of seismic energy or log of seismic moment can be substituted for the magnitude M (Han et al. 2015). The constants 'a' and 'b' describe both the productivity of a volume and slope of the frequency-magnitude distribution, quantifying the distribution of the events sizes. "b" is generally equals 1 approximately on the average, but "b" > 1 depicts small earthquakes, while "b" < 1 signifies predominant large earthquakes. The intercept and slope Log N against M plot usually gives the values of these constants. The size scaling of attributes of the seismicity are most times described by the b-values' statistical parameters and these values differ for different regions with ranges between 0.2 and 3.0. The b-value on an average regional scale is unity (1). The variation and perturbations in the b-value is linked to the stress type that characterize the region after main shocks (Ozturk, 2012). Lower b-values typify regions that are subjected to higher shear stress after main shocks, while higher b-values indicates region characterized with slip after main shocks. According to Ozturk (2012), high b-values also signify areas with complex geology that are characterized with multi-fractures. To an extent, low b-values indicate a low degree of heterogeneity within the cracked medium alongside large stress and strain with speedy deformations and large faults.

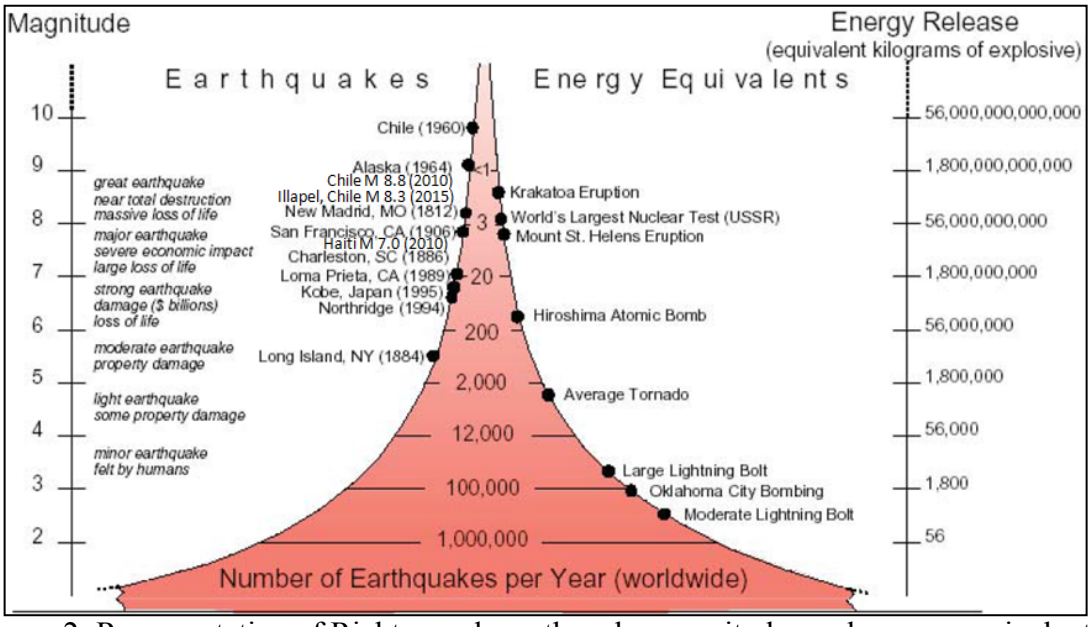

Figure 2: Representation of Richter scale earthquake magnitudes and energy equivalents. Source: Bravo and Ortiz (2005); Andrea et al. (2011).

The Maximum Likelihood Estimation (MLE) method is used to estimate the parameters of observations in statistical model, by estimating the parameter values that maximize the likelihood of making the observations given by the parameters. There are two mostly used methods in **b**-value estimation: least square and MLE methods, which have been adopted in this study. Provided that Eq. (1) exists, the Probability Density Function (PDF) of M is given as:

$$p(M) = b\ln(10)\frac{10^{-bM}}{10^{-bM_{\min}} - 10^{-bM_{\max}}} \quad (2)$$

where M_{max} and M_{min} are the maximum and minimum allowable magnitudes. Suppose that $M_{max} >> M_{min}$, then, Eq. (2) is rewritten as:

$$p(M) = b\ln(10)10^{-b(M-M_{\min})} \quad (3)$$

It is imperative to state that transition from Eq. (2) to Eq. (3) entails that the GR law exists for a range of magnitudes $M_{max} - M_{min} \geq 3$ (Aki, 1965). Before the MLE in Eq. (3) can be satisfied, **b**-value needs to be chosen such that it maximizes the likelihood function (Fisher, 1950) as given in Eq. (4).

$$b = \frac{1}{\ln(10)\left(\mu - M_{thresh}\right)} \quad (4)$$

where M_{thresh} and μ are the threshold magnitude and the sampling average of the magnitudes respectively. The M_{thresh} in most of the time corresponds to the minimum magnitude for the completeness of the seismic catalogue.

3.0 RESULTS AND DISCUSSION

3.1 Earthquakes' frequency-magnitude distribution

Earthquakes' magnitude distribution (M_d) is usually parameterized using GR power law relationship (Gutenberg and Richter, 1944). The annual distributions of events in the investigated period are presented in Table 2. The magnitude 5.0 to 5.9 shared 92.6% of the total earthquakes in the entire events. The minimum frequency of 27 recorded for this range occurred in the year 1964, while the maximal frequency of 435 recorded occurred in the year 2010. The magnitudes 6.0 to 6.9 shared 6.8%, 7.0 to 7.9 shared 0.6%, and 8.0 to 8.9 shared 0.1% of the total earthquakes of 3, 893. Basically, the magnitudes 5.0 – 5.9 were the most frequent with total events of 3,606, followed by magnitudes 6.0 – 6.9 with total events of 265, followed by magnitude 7.0 – 7.9 with total events of 25, and the least frequent but the highly devastating magnitude 8.0 – 8.9 showed overall occurrence of 4 events (with each event in year 2001, 2010, 2014 and 2015). This suggests that though light earthquakes

dominated the study area, recurring strike of these light earthquakes on the plates has triggered moderate, strong, major, and great earthquake occurrence in Chile especially a great earthquake which occurred in year 2014 and 2015 consecutively. This occurrence might trigger great tsunamis/earthquakes in some decades to come.

Table 2: Annual events of earthquake occurrences from 1964 – 2015.

Year/Magnitude	5-5.9	6-6.9	7-7.9	8-8.9	Total
1964	27	4	0	0	31
1965	48	4	2	0	54
1966	45	1	1	0	47
1967	32	4	0	0	36
1968	35	0	0	0	35
1969	24	3	0	0	27
1970	59	7	0	0	59
1971	75	5	0	0	80
1972	46	2	0	0	48
1973	71	6	0	0	77
1974	59	1	1	0	61
1975	45	3	1	0	49
1976	63	2	0	0	65
1977	112	4	1	0	117
1978	61	1	0	0	62
1979	72	3	0	0	75
1980	39	3	0	0	42
1981	42	3	0	0	45
1982	54	1	0	0	55
1983	76	2	1	0	79
1984	54	2	0	0	56
1985	137	7	2	0	146
1986	59	1	0	0	60
1987	80	6	1	0	87
1988	96	6	0	0	102
1989	52	1	0	0	53
1990	50	2	0	0	52
1991	49	1	0	0	50
1992	65	1	0	0	66
1993	44	6	1	0	51
1994	45	4	0	0	49
1995	67	4	1	0	72
1996	24	3	0	0	27
1997	50	10	2	0	62
1998	47	7	1	0	55
1999	31	7	0	0	38
2000	30	4	1	0	35
2001	119	9	1	1	130
2002	48	6	0	0	54
2003	46	3	0	0	49
2004	51	5	0	0	56
2005	44	2	1	0	47

2006	75	9	0	0	84
2007	119	10	1	0	130
2008	53	6	0	0	59
2009	59	4	0	0	63
2010	435	29	1	1	466
2011	102	11	1	0	114
2012	70	6	1	0	77
2013	54	4	1	0	59
2014	148	11	1	1	161
2015	118	19	1	1	139
Total	3606	265	25	4	3893

As revealed in Table 3, the time interval of 4 years (i.e. 1964 – 1967, 1968 – 1971, 1972 – 1975…2012 – 2015) was used. The earthquakes depicted a fluctuating trend in nature, but increases greatly towards the last 8 years of the events (i.e. 2008 – 2011 and 2012 – 2015). It is observed that every minimal point on the trend was the result of increase in magnitude of the earthquake (i.e. either occurrence of magnitude 6.0-6.9, 7.0-7.9, or 8.0-8.9). This shows that the previous 4-year earthquake events in Chile would have impact on the relative motion of the plates in Chile, which could lead to increase in accumulation of tectonic stress in the study area. The rate at which the magnitudes from 6.0-6.9, 7.0-7.9, and 8.0-8.9 increase suggests that the probability of a devastating earthquake is on the increase in the study area. The 2008-2011 interval produced the highest number of earthquakes (702 events), while that of 2012-2015 interval produced the second highest number of earthquakes (436 events) in the study area. This further suggests that Chile is currently seismically active and has tendency to produce more devastating incidence in years to come (for example, the interval 2016 – 2019, 2020 – 2023 and so on) with magnitude ranging between 6.0 and 8.9. However, Figure 3, revealed a more comprehensive trend of the overall number of earthquakes at 4-year interval. The graph showed a very high trend of earthquakes in the recent time (i.e. the last eight years).

Table 3: Variation of seismicity at interval of 4-year

Year/Mag.	**5-5.9**	**6-6.9**	**7-7.9**	**8-8.9**	**Total**
1964-1967	152	13	3	0	168
1968-1971	186	15	0	0	201
1972-1975	221	12	2	0	235
1976-1979	308	10	1	0	319
1980-1983	211	9	1	0	221
1984-1987	330	16	3	0	349
1988-1991	247	10	0	0	257
1992-1995	221	15	2	0	238
1996-1999	152	27	3	0	182
2000-2003	243	22	2	1	268
2004-2007	289	26	2	0	317
2008-2011	649	50	2	1	702
2012-2015	390	40	4	2	436

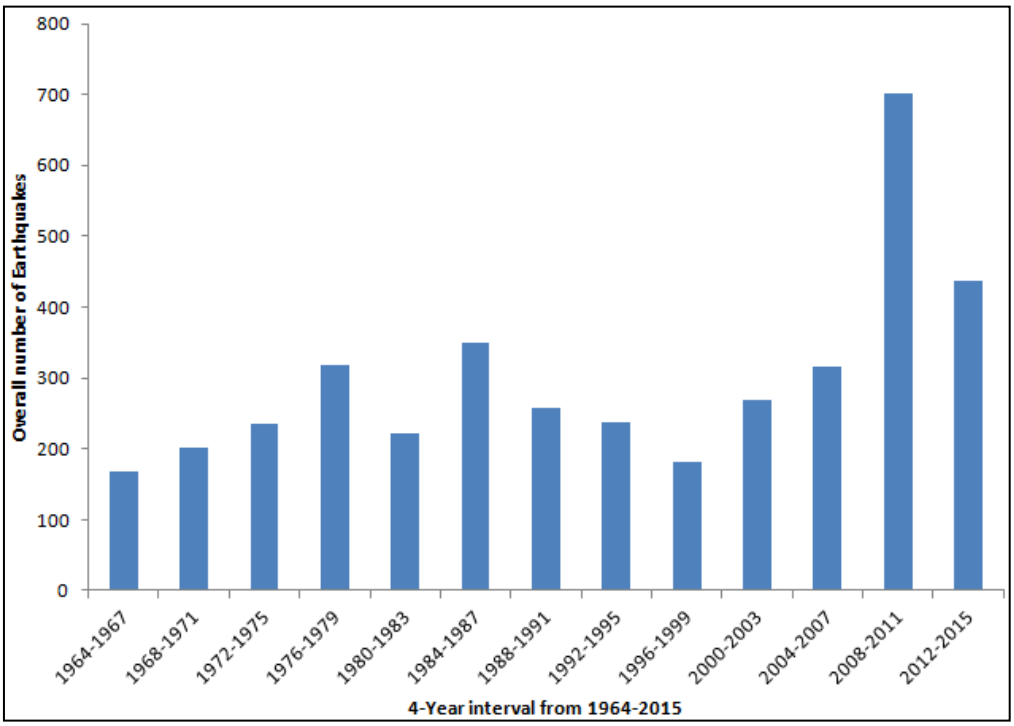

Figure 3: Overall number of earthquakes M 5.0 at 4-year interval in Chile (1964-2015).

The central tendency was also performed on the data used in order to obtain average magnitude and focal depth as well as spread and relative frequencies of the data set. However, the descriptive statistics (Table 4) were computed both for the magnitudes and the focal depths of the events in order to obtain the relative frequencies and the trend of the data set. The results revealed that the average magnitude of the data set was 5.3 (light earthquake which results in some property damage) while the average focal depth was 68.7 km (shallow earthquake depth). The modal values of the focal depth and magnitudes are 33.0 and 5.0 respectively. This indicates that most of the earthquakes occurred within the lithosphere.

The total seismic events of shallow earthquake depth were 2,488 while that of intermediate earthquake depth were 1,401 events. The crustal earthquakes (f <40 km) recorded were 1,910 events while that of upper mantle region (f >40 km) were 1,971 events. The standard deviation of 0.4 was computed for the all the magnitudes. This implies that seismic events in the study area have a significant spread. Though the shallow earthquake depth events are greater than the intermediate earthquake depth in the study area, moderate-to-great earthquake of intermediate depth still occur in Chile.

As revealed in Table 3, the time interval of 4 years (i.e. 1964 – 1967, 1968 – 1971, 1972 – 1975…2012 – 2015) was used. The earthquakes depicted a fluctuating trend in nature, but increases greatly towards the last 8 years of the events (i.e. 2008 – 2011 and 2012 – 2015). It is observed that

every minimal point on the trend was the result of increase in magnitude of the earthquake (i.e. either occurrence of magnitude 6.0-6.9, 7.0-7.9, or 8.0-8.9). This shows that the previous 4-year earthquake events in Chile would have impact on the relative motion of the plates in Chile, which could lead to increase in accumulation of tectonic stress in the study area. The rate at which the magnitudes from 6.0-6.9, 7.0-7.9, and 8.0-8.9 increases suggests that the probability of a devastating earthquake is greater in the study area. The 2008-2011 interval produced the highest number of earthquakes (702 events), while that of the 2012-2015 interval produced the second highest number of earthquakes (436 events) in the study area. This further suggests that Chile is currently seismically active and has tendency to produce more devastating incidence in years to come (for example, the interval 2016 – 2019, 2020 – 2023 and so on) with magnitude ranging between 6.0 and 8.9. However, Figure 3, revealed a more comprehensive trend of the overall number of earthquakes at 4-year interval. The graph showed a very high trend of earthquakes in the recent time (i.e. the last eight years).

Table 4: Basic descriptive statistics of the events.

	Depth	Magnitude
Mean	68.7	5.3
Mode	33.0	5.0
Median	41.0	5.2
Standard Deviation	--	0.4

3.2 Trend analysis

Another form of examining data is through the analysis of its trend. The trend analysis was achieved by constraining the time series (moving average) on the graph of earthquake frequencies against the annual distribution of the events. The 3-point moving average was employed to decompose the time series into random, seasonal or cyclic trend variations. It could also occur as more than one variation. The results are presented in Figures 4a to 4d. The line graphs showed that the observed magnitudes ranged for about 52 years. They depict the pictures of earthquake frequency distribution with varying ranges of magnitudes. The three-point-moving average for Chile behaves approximately like the line graphs when contrasted. The rates of seismicity anomalies in Chile for all the magnitude ranges are irregular or fluctuating. The seismicity studies from previous works reported that Chile is one of the few places where three major plates (triple junction) meet (Leyton et al. 2009; Martinez-Alvarez et al. 2013; Kato et al. 2016). This suggests that Chile is seismically active which has been revealed in this study.

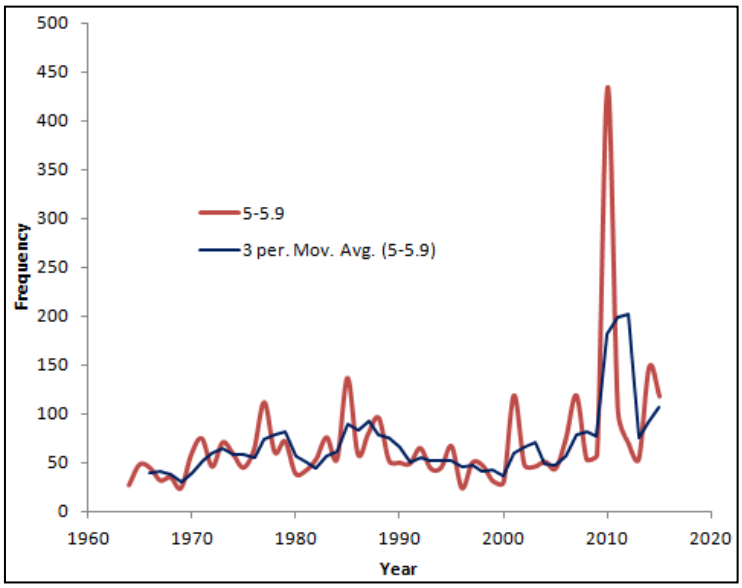

Figure 4a: Trend analysis of $5.0 \leq M \leq 5.9$ earthquakes.

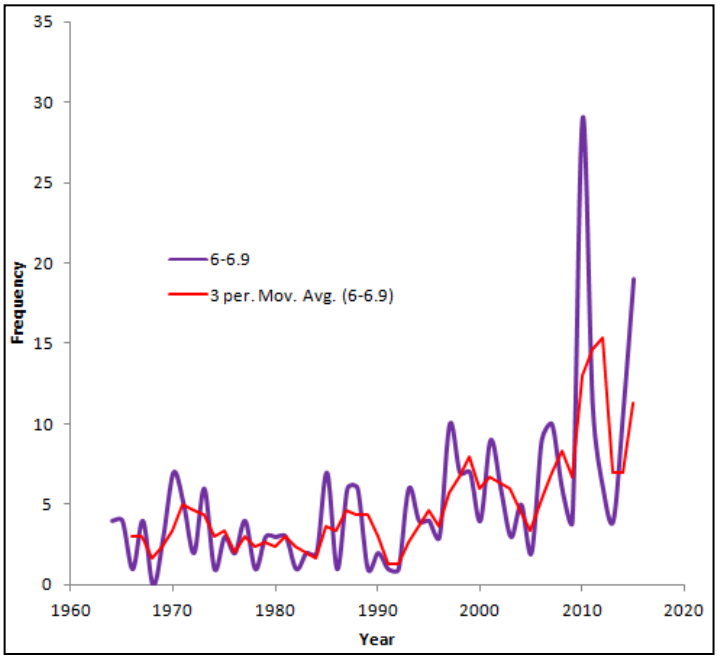

Figure 4b: Trend analysis of $6.0 \leq M \leq 6.9$ earthquakes.

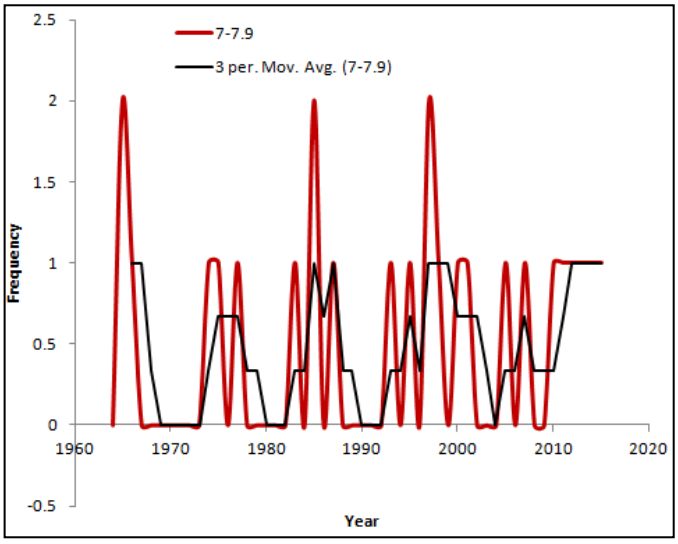

Figure 4c: Trend analysis of $7.0 \leq M \leq 7.9$ earthquakes.

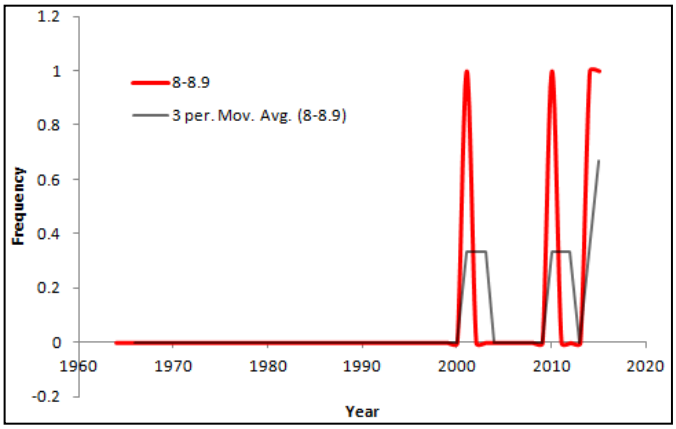

Figure 4d: Trend analysis of $8.0 \leq M \leq 8.9$ earthquakes.

The 3,893 events in Chile for 52 years (1964 – 2015) were presented in 3-D form (Figure 5). It was revealed that the analysis of the natural hazards in the study area opened our understanding about the geodynamic process of the plate collision that has been attributed to the movement of the triple junction around Chile. The great earthquake (M_W 8.3) that occurred in Illapel on September 16, 2015 falls towards the central portion of the study area (latitude 31^o $38^{'}$ $00^{"}$ S and longitude 71^o $10^{'}$ $10^{"}$ W) where clusters of moderate-to-great earthquakes have been experienced. Only SW of the study area showed to be freed from M 6.0 earthquakes. This reveals how seismically active Chile and its vicinity has been.

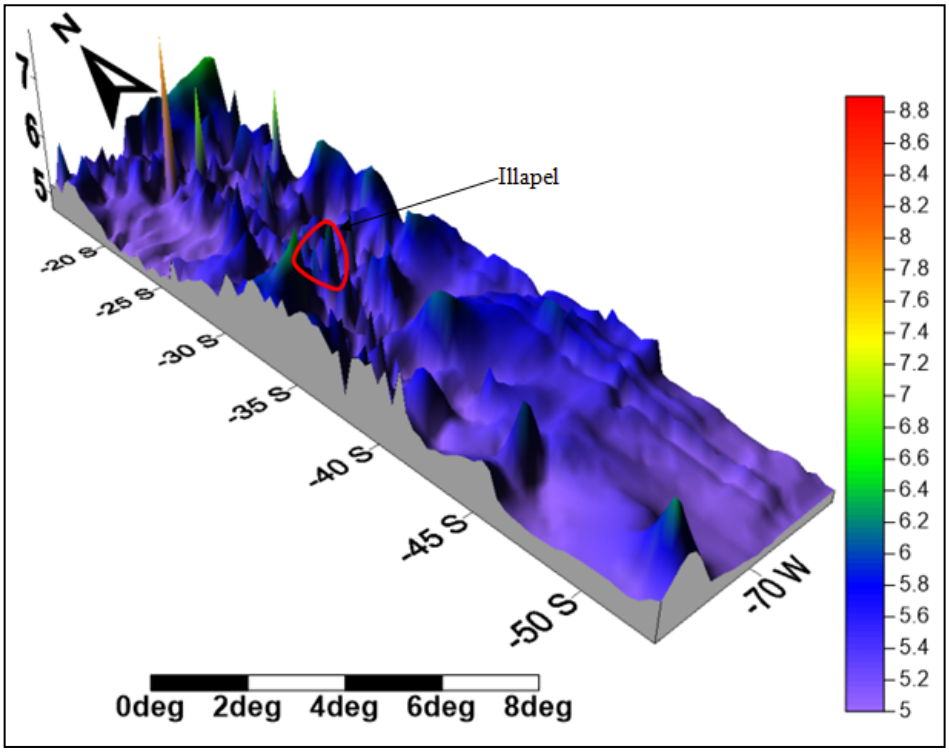

Figure 5: 3-D plot M 5.0 earthquakes in Chile and its vicinity for the period of 1964-2015

3.3 b-value Estimation

Two methods were adopted to estimate the **b**-value in this study: GR and MLE, due to its significance in seismology. Earthquake frequency-magnitude relation is one of the ways to describe and analyze the seismic activity in an area (Schwartz and Coppersmith, 1984; Darwin, 1845; Ghosh, 2007; Adagunodo et al. 2018), the exponential model that implies that earthquakes on a given fault follow the G-R model. The **a**-value and **b**-value in the G-R power law are parameters that supply essential information in seism tectonic studies and seismic risk analysis; hence their correct computation reveals important information on seismology of an area.

The magnitude of completeness (M_C) for the data set is 4.5, based on the Magnitude-Frequency Distribution (MFD) assumption as depicted in Figure 6. The M_C represents the lowest magnitude at which 100 percent of the events in a space-time volume are determined (Han et al. 2015). The GR relation in Chile gives the productivity of a volume as 8.4. The **a**-value is a function of the quantity of earthquake occurrences in an area. However, the estimated **b**-value using GR and MLE methods are 0.97 and 1.1 respectively. The results from the two techniques show that the **b**-value in Chile revolves round 1.0. The earthquakes in the study area are considered as large, since the estimated **b**-value ≈ 1. This shows that Chile is seismically active. As reported by Alabi et al. (2013), that high stress implies low **b**-value. This has been revealed from the average focal depth of the study area,

which is characterized by shallow earthquake depth of 68.7 km as presented in Table 4. Furthermore, most of earthquakes occurrence in the study area occurred within the depth > 40 km (upper mantle region) which showed how highly stressed the plates in the study area have been. Though Alabi *et al*. (2013) reported that the **b**-value so far have not been really understood from the previous researches, it has been the major yardstick to categorize seismic occurrence in a region to either small (b>1) or large (b<1) earthquakes.

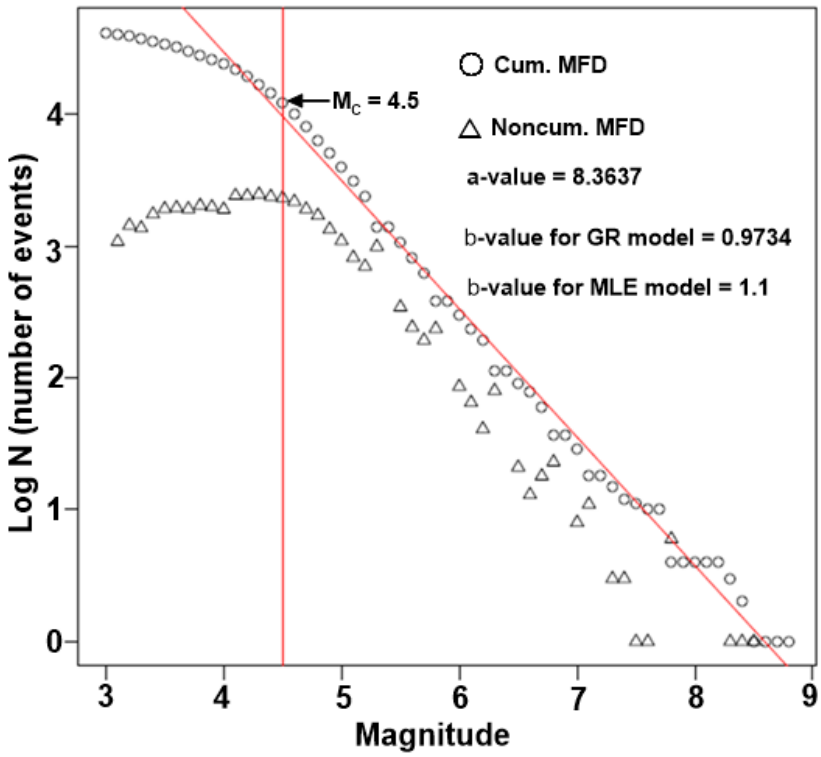

Figure 6: The MFD plot of earthquake occurrence in Chile from 1964 – 2015.

4.0 CONCLUSION

Chile can be regarded as seismically active zone due to the movement of the plates (especially the three plates that meet) in this region. Chile is one of the interplate seismic zones globally, which record had shown that the region has been experiencing earthquakes since 1570. However, an interplate earthquake is one that occurs at plate boundary. The surface of the Earth is made up of seven primary and eight secondary tectonic plates, with dozens of tertiary micro plates. The large plates move very slowly, owing to convection currents within the mantle below the crust. Because they do not all move in the same direction, plates often directly collide or move laterally along each other, a tectonic environment that makes earthquakes frequent. Relatively, few earthquakes occur in intraplate (an earthquake that occurs in the interior of a tectonic plate) environments; most occur on faults near plate margins. Scientists continue to search for the causes of earthquakes, and especially for some indication of how often they recur.

Based on all the approaches used for this study, it can be concluded that Chile is prone to recurrence of moderate-to-great earthquakes in the future. This implies that the probability that a large earthquake would recur in Chile is very high. Though Chilean government has legalized Chile's strict building code (the country's building codes require that all new buildings must be able to survive a 9.0-magnitude earthquake), but not for a very severe earthquake like the one recorded in 1960 M_w 9.5 earthquake, which occurred in southern Chile. Since earthquakes and tsunamis are deadly natural phenomena, Chilean government should prepare for any future occurrence of an earthquake greater than magnitude M_w 9.0.

ACKNOWLEDEMENTS

The authors are eminently grateful to the management of Covenant University, Nigeria for the publication support received from them. The authors are grateful to the Northern California Earthquakes Data Centre–a joint project of the University of California Berkley Seismological laboratory and of the U.S. Geological Survey (USGS) for providing the data that was used for this study. Also, the contributions of Advanced Natural Seismic Source (ANSS) for accessing the data are highly appreciated.

REFERENCES

Abe K. (1979). Size of great earthquakes of 1837 – 1974 inferred from tsunami data. Journal of Geophysical Research, 84(B4): 1561 – 1568. https://doi.org/10.1029/JB084iB04p011561.

Abercombie R.E. (1995). Earthquake source scaling relationships from -1 to 5 M_L using seismograms recorded at 2.5 km depth. J. Geophys. Res., 100: 24015-24036.

Adagunodo T.A. and Sunmonu L.A. (2015). Earthquake: a Terrifying of all Natural Phenomena. Journal of Advances in Biological and Basic Research. 01(1): 4–11.

Adagunodo T.A., Lüning S., Adeleke A.M., Omidiora J.O., Aizebeokhai A.P., Oyeyemi K.D., Hammed O.S. (2018). Evaluation of $0 \leq M \leq 8$ Earthquake Data Sets in African-Asian Region during 1966 – 2015. Data in Brief, 17C: 588 – 603. https://doi.org/10.1016/j.dib.2018.01.049.

Aida I. (1978). Reliability of Tsunami Source Model derived from Fault Parameters. J. Phys., Earth, 57 – 73.

Aki M. (1965). Maximum likelihood estimate of b in the formula Log (N) = a – bM and its confidence limits. Bull. Earthq. Res. Inst. Tokyo Univ., 43: 237 – 239.

Alabi A.A., Akinyemi O.D. and Adewale A. (2013). Seismicity pattern in Southern Africa from 1986 to 2009. Earth Science Research, 2(2): 1-10.

Andrea A., Piero B. and Fabio G.T. (2011). Earthquake damage assessment based on remote sensing data. The Haiti case study. Italian Journal of remote sensing, 43(2): 123-128.

Awoyemi M.O., Hammed O.S., Shode O.H., Olurin O.T., Igboama W.N., Fatoba J.O. (2017). Investigation of b-value variations in the African and parts of Eurasian plates. Journal of Tsunami Society International, 36(2): 86 – 99.

Awoyera P. O., Ogundeji J. and Aderonmu P.A. (2016). Simulated Combined Earthquake and Dead Load Lateral Resistance Building Systems using Nigeria Seismic Data. *Journal of Materials and Environmental Science, 7 (3): 781-789. ISSN 885-894*

Awoyera P.O., Ngene B.U., Adeyemi G.A., Aderonmu P.A. (2017). *Mitigating Ground Shaking Construction Activities in Coastal Cities of Nigeria: An Earthquake Preventive Measure. In: Earthquakes: Monitoring Technology, Disaster Management and Impact Assessment. Nova Science Publishers, Inc.. ISBN 978-1536103427*

Bolshakova A.V., Nosov, M.A. (2011). Parameters of tsunami source versus earthquake magnitude. Pure Appl. Geophys., 168: 2023 – 2031. doi:10.1007/s00024-011-0285-3

Bravo T.K. and Ortiz A.M. (2005). Plotting earthquake epicenters: an activity for seimic discovery. Science education solutions, 1-14.

Cox, D.C. and Pararas-Carayannis, G. 1968. A Catalog of Tsunamis in Alaska. Data Report Hawaii Inst.Geophys. Mar. 1968.

Darwin C. (1845). The voyage of the Beagle (1975 Reissue). London: J.M. Dent.

Dzierma Y., Thorwart M., Rabbel W., Siegmund C., Comte D., Bataille K., Iglesia P. and Prezzic (2012). Seismicity near the slip maximum of the 1960 Mw 9.5 Valdivia earthquake (Chile): plate interface lock and reactivation of the subducted Valdivia fracture zone. J. Geophys. Res., 117, B06312, 1-13.

El-Isa Z.H. and Eaton D.W. (2014). Spatiotemporal variations in the b-value of earthquake magnitude-frequency distributions: classification and causes. Technophysics, 615 – 616: 1 – 11.

Fisher R.A. (1950). Contribution to mathematical statistics. New York: Wiley.

Ghosh A. (2007). Earthquake frequency-magnitude distribution and interface locking at the Middle America subduction zone near Nicoya Peninsula, Costa Rica. Georgia Institute of Technology. http: //smartech.gatech.edu/handle/1853/16288.

Gutenberg B. and Richter C.F. (1944). Frequency of earthquakes in California. Bull. Seismol. Soc. Am., 34, 185-188.

Hammed O.S., Popoola O.I., Adetoyinbo A.A., Awoyemi M.O., Adagunodo T.A., Olubosede O., Bello A.K. (2018). Peak Particle Velocity Data Acquisition for Monitoring Blast Induced Earthquakes in Quarry Sites. Data in Brief, 19: 398 – 408. https://doi.org/10.1016/j.dib.2018.04.103.

Han Q., Wang L., Xu J., Carpinteri A., Lacidogna G. (2015). A robust method to estimate the b-value of the magnitude – frequency distribution of earthquakes. Chaos, Solitons and Fractals, 81: 103 – 110.

Ismail-Zadeh A., Soloviev A., Sokolov V., Vorobieva I., Muller B., Schilling F. (2017). Quantitative modeling of the lithosphere dynamics, earthquakes and seismic hazard. Tectonophysics, http://dx.doi.org/101016/J.tecto.2017.04.007

Iida, K., D.C. Cox, and Pararas--Carayannis, G., 1967. Preliminary Catalog of Tsunamis Occurring in the Pacific Ocean. Data Report No. 5. Honolulu: Hawaii Inst.Geophysics, Aug. 1967.

Kanamori, H. & J.J. Cipar, 1974. Focal Process of the Great Chilean Earthquake of May 22, 1960. Physics of the Earth and Planetary Interiors, 9 (1974) 128~136, North-Holland Publishing Company, Amsterdam

Kato A., Fukuda J., Kumazawa T. and Nakagawa S. (2016). Accelerated nucleation of the 2014 Iquique, Chile M_W 8.2 earthquake. Scientific Reports, 6: 24792. DOI: 10:1038/srep24792.

Lander, J. F. and Lockridge, P. A., 1989, United States Tsunamis (including United States possessions) 1690-1988: U.S. Dept. of Commerce, National Oceanic and Atmospheric Administration, 265 p..

Lay T., Yamazaki Y., Ammon C.J., Cheung K.F. and Kanamori H. (2011). The 2011 Mw 9.0 off the Pacific coast of Tohoku earthquake: Comparison of deep-water tsunami signals with finite-fault rupture model predictions. Earth Planets Space, 63(7): 797 – 801. doi:10.5047/eps.2011.05.03.

Leyton F., Perez A., Campos J., Rauld R., Kausel E. (2009). Anomalous seismicity in the lower crust of the Santiago Basin, Chile. Physics of the Earth and Planetary Interiors, 175(1-2): 17 – 25.

Lin, Frank C. ; Sookhanaphibarn, Kingkarn; Choensawat, Worawat; and George Pararas-Carayannis. 2016. Detection of Tsunami Radiation at Illapel, Chile on 2015-0-16 by Remote Sensing. Journal of Tsunami Society International, Science of Tsunami Hazards, Vol. 35 No 1, 2016 http://www.tsunamisociety.org/STHVol35N1Y2016.pdf

Martinez-Alvarez F., Reyes J., Morales-Esreban A., Rubio-Escudero C. (2013). Determining the best set of seismicity indicators to predict earthquakes. Two case studies: Chile and the Iberian Peninsula. Knowledge-Based Systems, 50: 198 – 210.

Nava F.A., Marquez-Ramirez V.H., Zuniga F.R., Avila-Banientos L., Quinteros C.B. (2017). Gutenberg – Richter b-value maximum likelihood estimation and sample size. J. Seismol., 21: 127 – 135.

Nuannin P., Kulhanek O., Persson L. (2012). Variations of b-values preceding large earthquakes in the Andaman-Sumatra subduction zone. Journal of Asian Earth Sciences, 61: 237 – 242.

Olokoyo F.O., George T.O., Efobi U.R., Beecroft I. (2017). Land deals and sustainable income: The case of a rural community in Ogun state, Nigeria. In: Natural Resources Management Concepts, Methodologies, Tools, and Applications, 2-2: 1004 – 1019. ISBN: 9781522508038.

Ozturk S. (2012). Statistical correlation between b-value and fractal dimension regarding Turkish epicenter distribution. Earth Science Research Journal, 16(2): 1-10.

PalamaTalukdar (2014). Preparation of a comprehensive earthquake catalogue for Northeast India and its completeness analysis. IOSR Journal of Geology and Geophysics, 6(1), 22-26.

Pararas-Carayannis, G., 1968a, Catalog of Tsunamis in the Hawaiian Islands. Hawaii Inst.Geophysics Report. Jan. 1968.

Pararas-Carayannis, G., 1968b. Tsunami Height Report, World Data Center A -Tsunami Report 1968.

Pararas-Carayannis, George, 1969. Chile Earthquake and Tsunami of 22 May 1960. Catalog of Tsunamis in the Pacific Ocean and for the Catalog of Tsunamis in the Hawaiian Islands. World Data Center A- Tsunami U.S. Dept. of Commerce Environmental Science Service Administration Coast and Geodetic Survey, May 1969). http://www.drgeorgepc.com/Tsunami1960.html

Pararas-Carayannis George, 2010 a. Chile Earthquake and Tsunami of 27 February 2010 - Evaluation Evaluation of Source Mechanism and of Near and Far-field Tsunami Effects. Tsunami Society International' Journal "Science of Tsunami Hazards", Vol. 29, No. 2, pp. 96-126 (2010) http://www.drgeorgepc.com/Tsunami2010Chile.html

Pararas-Carayannis George, 2010 b. Haiti – The earthquake of 12 January 2010. http://www.drgeorgepc.com/Earthquake2010Haiti.html

Pararas-Carayannis, G., 2012. Geodynamics of Nazca ridge's oblique subduction and migration - implications for tsunami generation along central and southern Peru: Earthquake and Tsunami of 23 June 2001. Science of Tsunami Hazards, Vol 31, No. 2, pp. 129-153, 2012 http://www.tsunamisociety.org/STHVol35N1Y2016.pdf

Prasad R. (2010). Chile: where three tectonic plate boundaries meet. www.thehindu.com/sci-tech/energy-and-environment, article 139026.ece. Updated on March 5, 2010.

Reyes J., Morales-Esteban A., Martinez-Alvarez F. (2013). Neural networks to predict earthquakes in Chile. Applied Soft Computing, 13: 1314 – 1328.

Schwartz D.P. and Coppersmith K.J. (1984). Fault behaviour and characteristic earthquakes: examples from the Wasatch and San Andreas Fault Zone. J. Geophys. Res., 89: 5681-5698.

Silbergleit V. and Prezzi C. (2012). Statistics of major Chilean earthquakes recurrence. Nat. Hazards, 62(2): 445 – 458. doi: 10.1007/s11069-012-0086-8.

Talley Carroll Jr. H. and Cloud William K;1960; United States Earthquakes 1960, U.S. Department of Commerce, Coast and Geodectic Survey Report.

United States Geological Survey (2015). M 8.3-48 km W of Illapel, Chile. Retrieved on September 16, 2015.

WikiProject Earthquakes (2017). List of earthquakes in Chile. https://en.wikipedia.org/wiki/. Retrieved on December 17, 2017.

Yamashita T. and Sato R. (1974). Generation of Tsunami by a Fault Model. J. Phys. Earth, 22: 415 – 440.

Zaytsev O., Rabinovich A.B. and Thomson R.E. (2016). A comparative analysis of coastal and open-ocean records of the great Chilean tsunamis of 2010, 2014 and 2015 off the coast of Mexico. Pure and Applied Geophysics. doi:10.1007/s00024-016-1407-8.

Stauder, W., 1973. J. Geophys. Res., 78: 5033-5061

ISSN 8755-6839

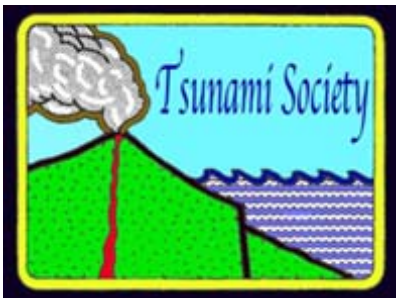

SCIENCE OF TSUNAMI HAZARDS

Journal of Tsunami Society International

Volume 37 Number 2 2018

TSUNAMI SOCIETY INTERNATIONAL, 1741 Ala Moana Blvd. #70, Honolulu, HI 96815, USA.

WWW.TSUNAMISOCIETY.ORG